

Quantum Dots and Self-assembled Q.dots-DNA Hybrids for Device Interface and Biosensor Applications.

S. N. Sahu

Institute of Physics
Bhubaneswar – 751007
E-mail:sahu@iopb.res.in

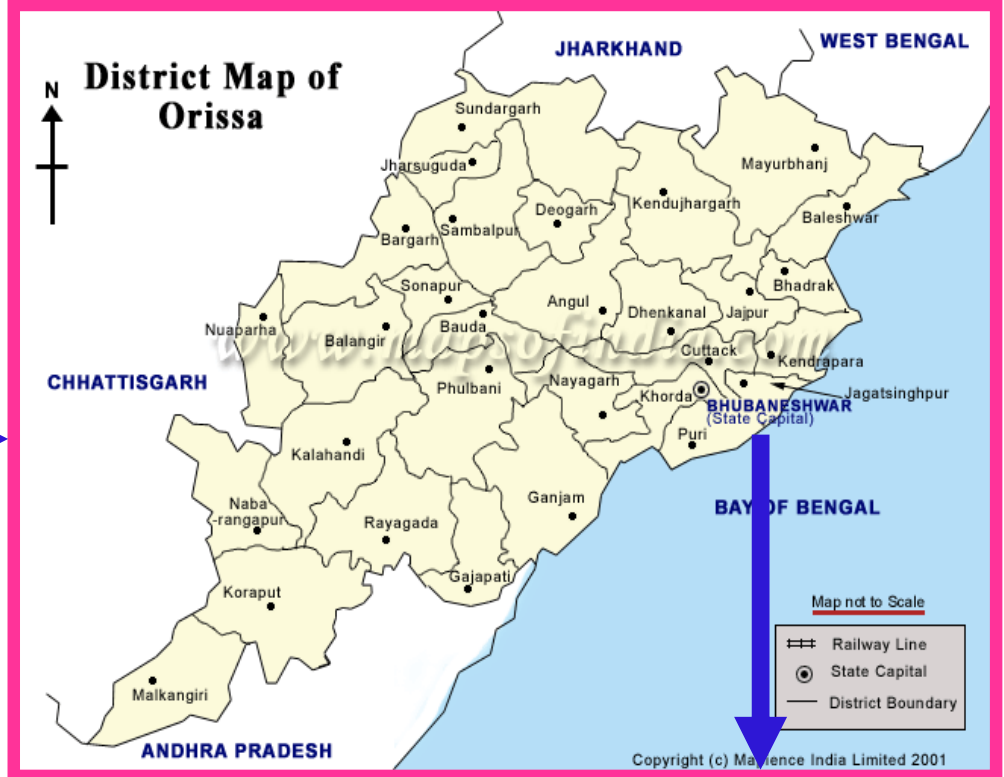
1. Introduction

2. Semiconductor
Nanocrystals

3. Nano-Bio systems

4. Applications

5. Conclusion



Nanostructure and cluster activities at Institute of Physics, Bhubaneswar

➤ Synthesis Routes

<u>Chemical</u>	<u>Electrochemical</u>	<u>Cluster</u>
Cds	CdSe GaAs Pbs HgS	Sb and Se
	HgTe and Porous Si	Sb ₂ O ₃ ,
	HgTe-DNA, CdSe-DNA	and SeO ₂ ,
	and bio-molecular	(LECBD)
	recognition	

Synthesis of nanostructures by solid-ion beam interaction by
Sputtering, ion implantation and MeV ion irradiation

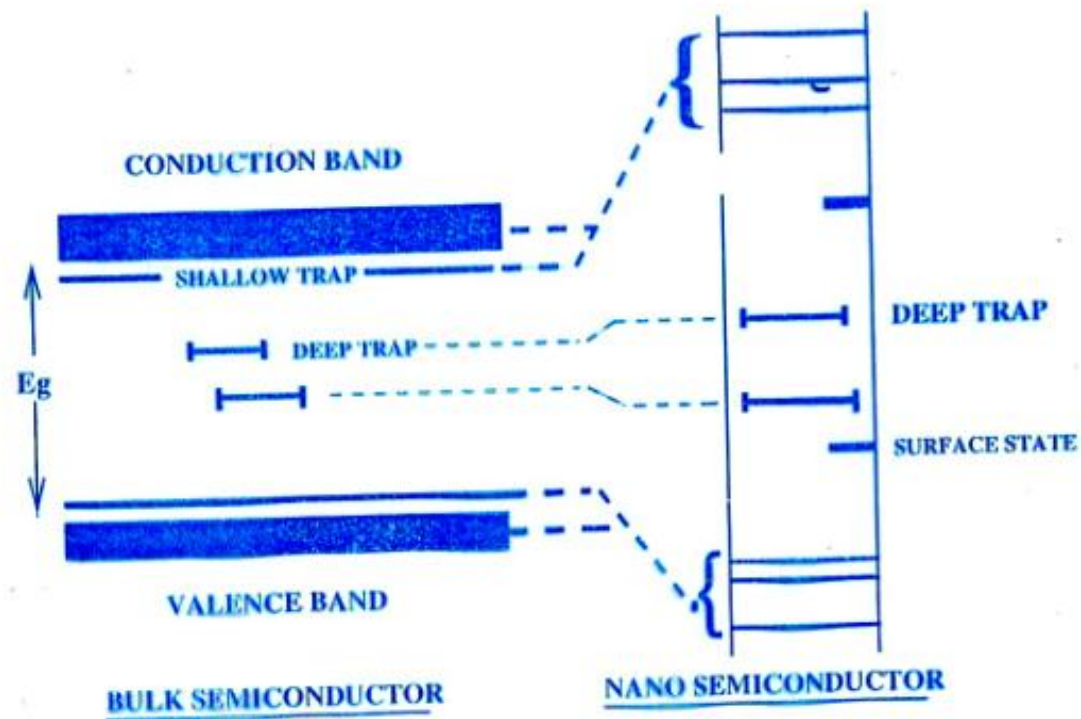
Theory: Electronic structure calculation

➤ Studies: Composition, thickness & impurity, Structure, size,
Surface, Optical, Device/ Interfacial, Electronic structure,
and Nano-bio systems

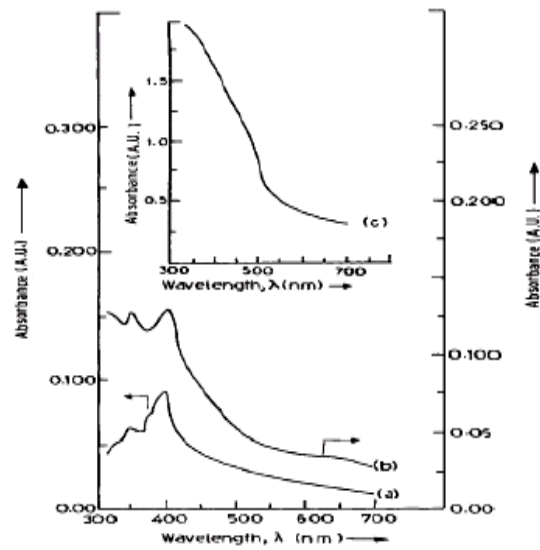
Facilities at IOP: Accelerator, GXRd, HRTEM, AFM/ MFM. XPS,
ARUPS, MBE, PL, Spectrophotometer, Raman,
FTIR, LCR meter, LECBD set up, Chemical Lab.
X-ray reflectivity, Langmuir,

Applications: Nano-Electronic Devices,
UV Sensor, Bio-molecular recognition

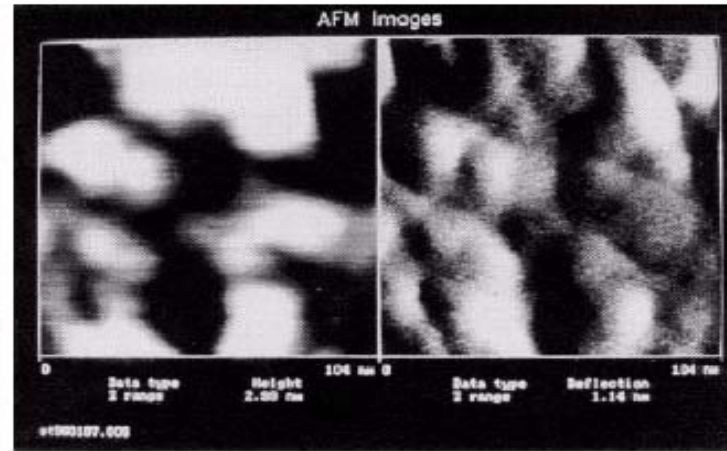
Energy Band Scheme for bulk and nanostructured semiconductors



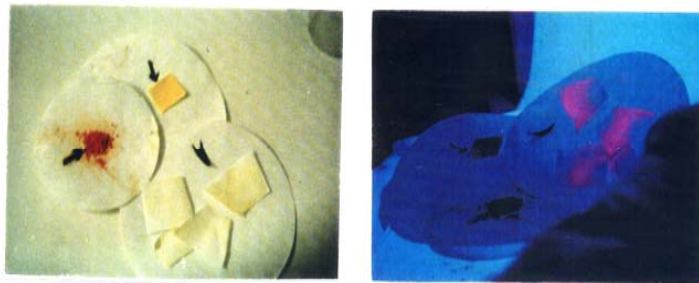
Nano-CdS



Optical absorption of CdS

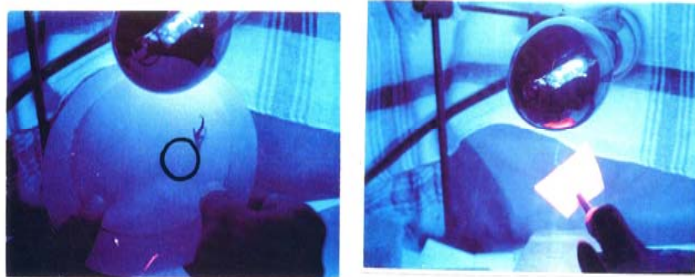


AFM of nano-CdS



(a)

(b)

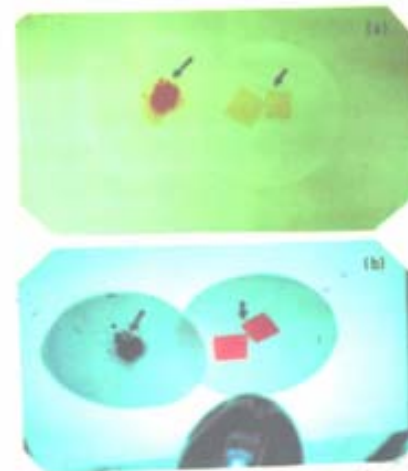


(c)

(d)

Visible light emission from CdS (a,b,c,d) and HgTe (a,b) under UV excitation

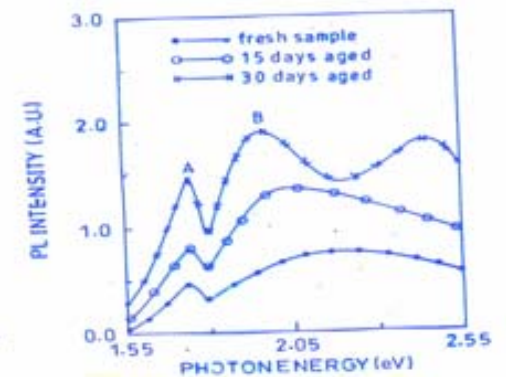
Acts as an UV sensor at room temperature



a)
b)

Under white light
Under UV light

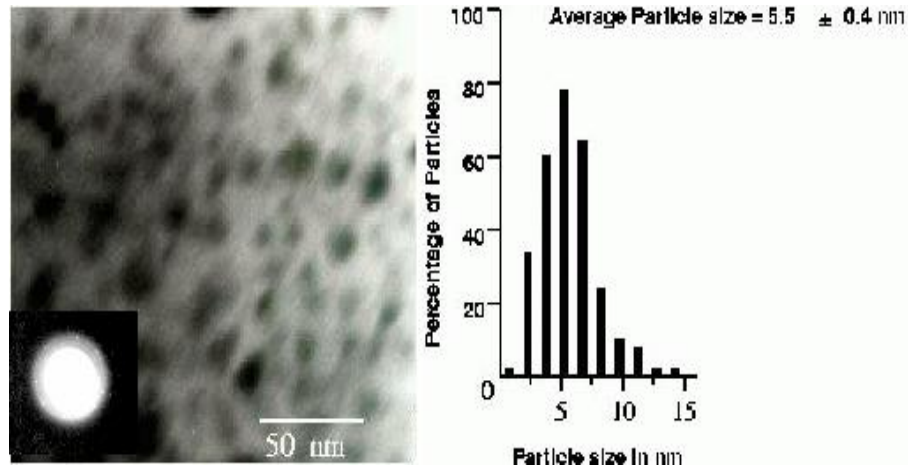
PL of CdS nanocrystals with aging effect



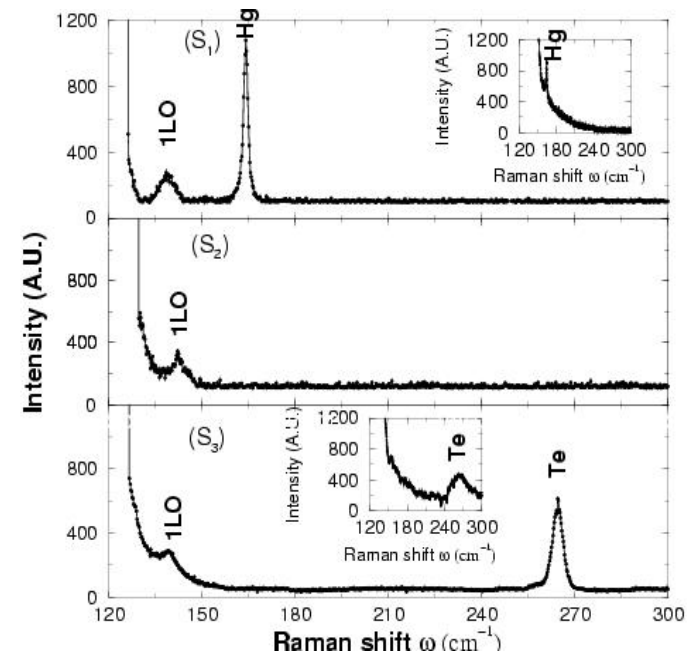
(c) New peaks appear with time. Deep trap positions (A) does not change with time where as shallow traps (B) move with increase in size- red shifted

Nano-HgTe

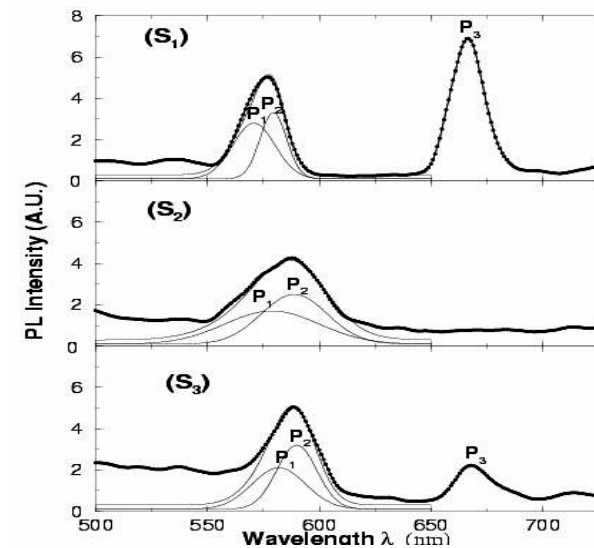
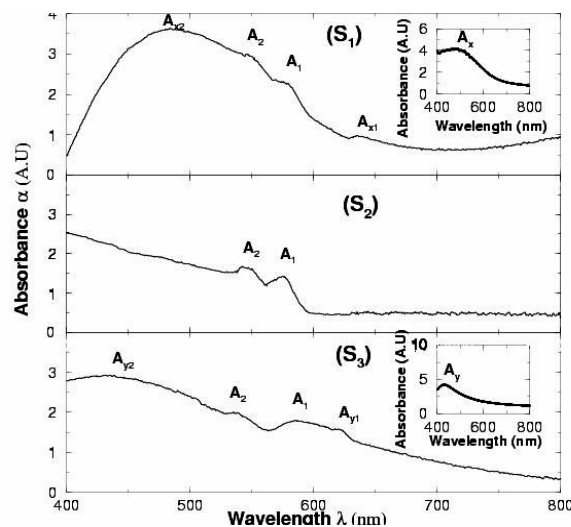
TEM Micrograph, SAD and histogram of HgTe Nanocrystals



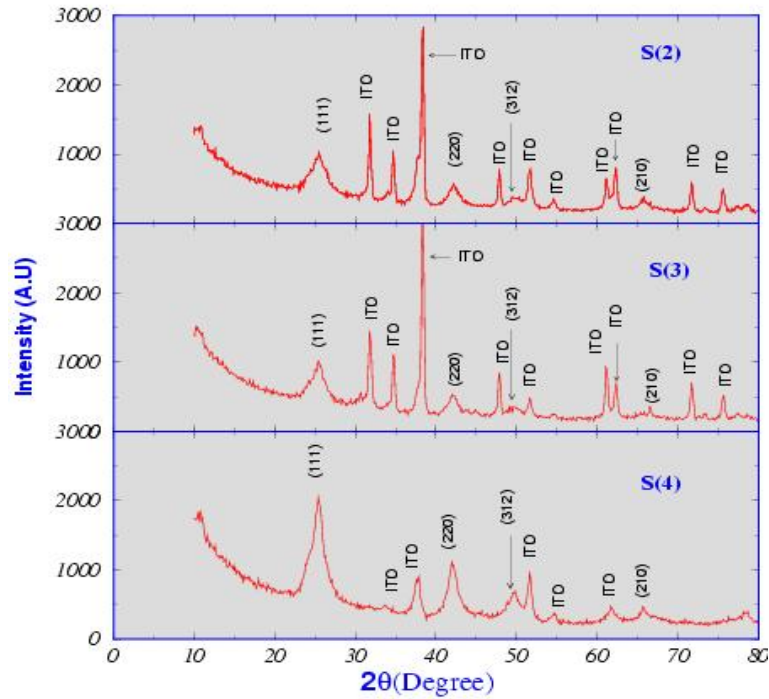
Compositional dependent micro Raman spectra of nano-HgTe



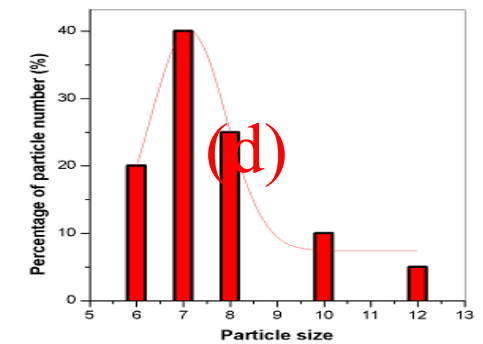
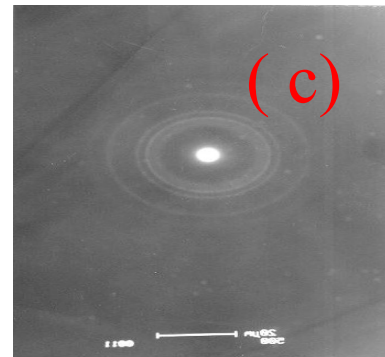
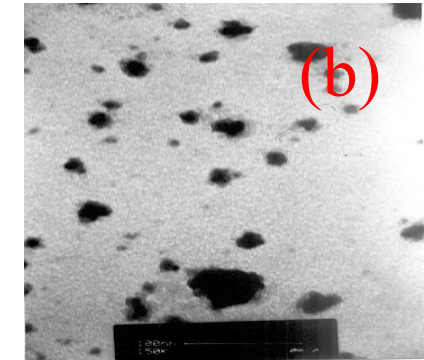
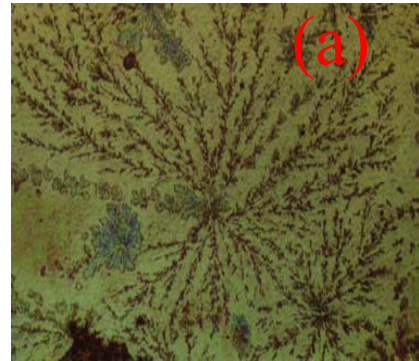
Composition dependent optical absorption and PL of HgTe Nanocrystal



Nano-CdSe



Glancing Angle X-ray
Diffraction (GAXRD) Spectra of
CdSe nanocrystals



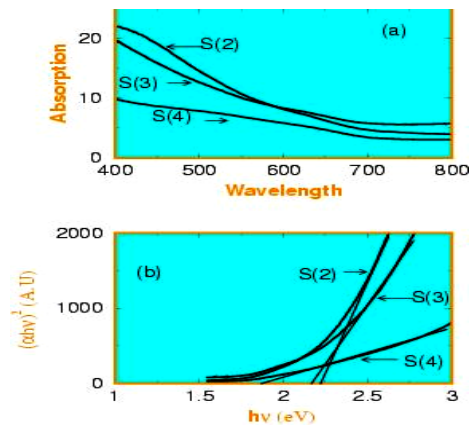
a) Fractal growth
DLA pattern
Dimension: 1.6

b) Micrograph

c) SAD: Cubic phase

Polycrystalline

d) Histogram:
Mean Size: 7.5 nm

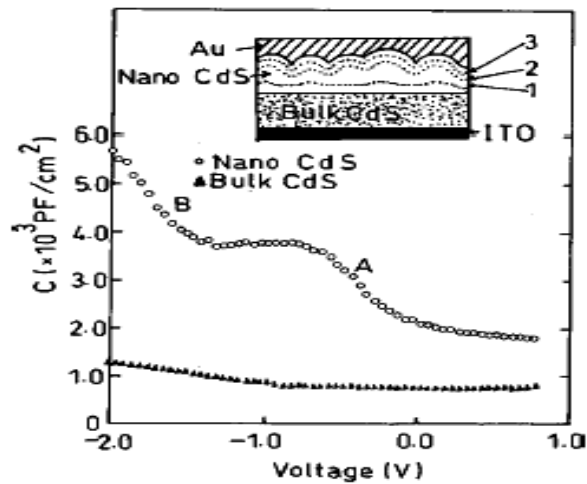
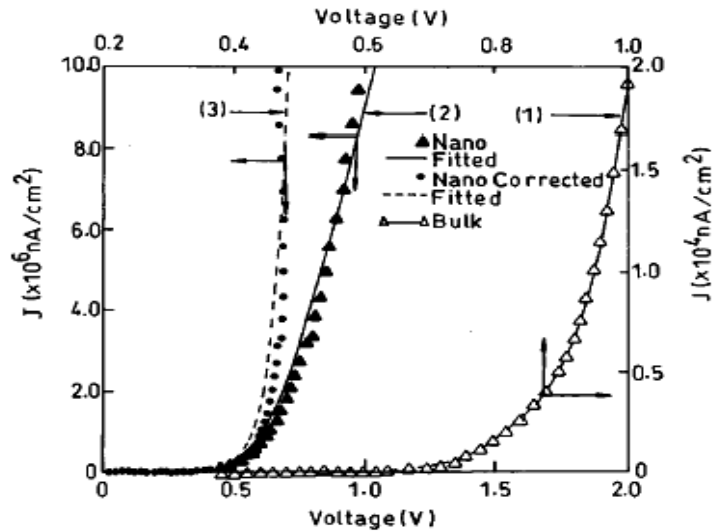


Sample S(2) (2.22 eV) is blue shifted
by 0.52 eV from it's standard bulk
value (1.7 eV)

Optical Absorption Spectra of CdSe Nanocrystals

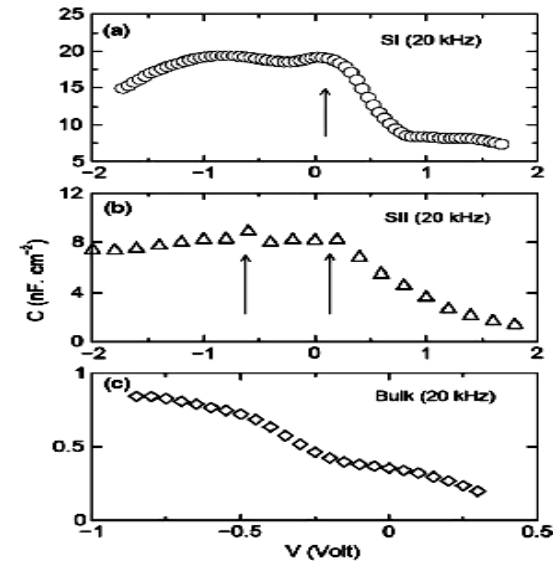
ITO/ bulk-CdS/ nano-CdS / Au device

I-V characteristic give series

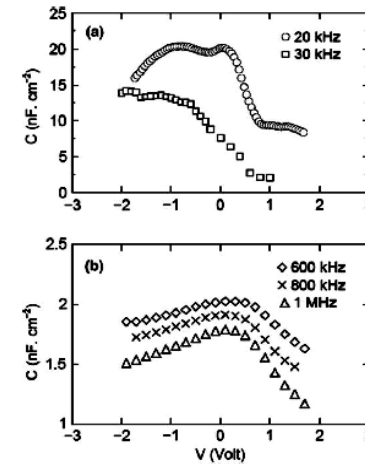


C-V characteristics of nano-CdS/Au and bulk-CdS/Au junctions at frequency of 1 kHz.

Au/Ga₂O₃/GaAs MOS structure

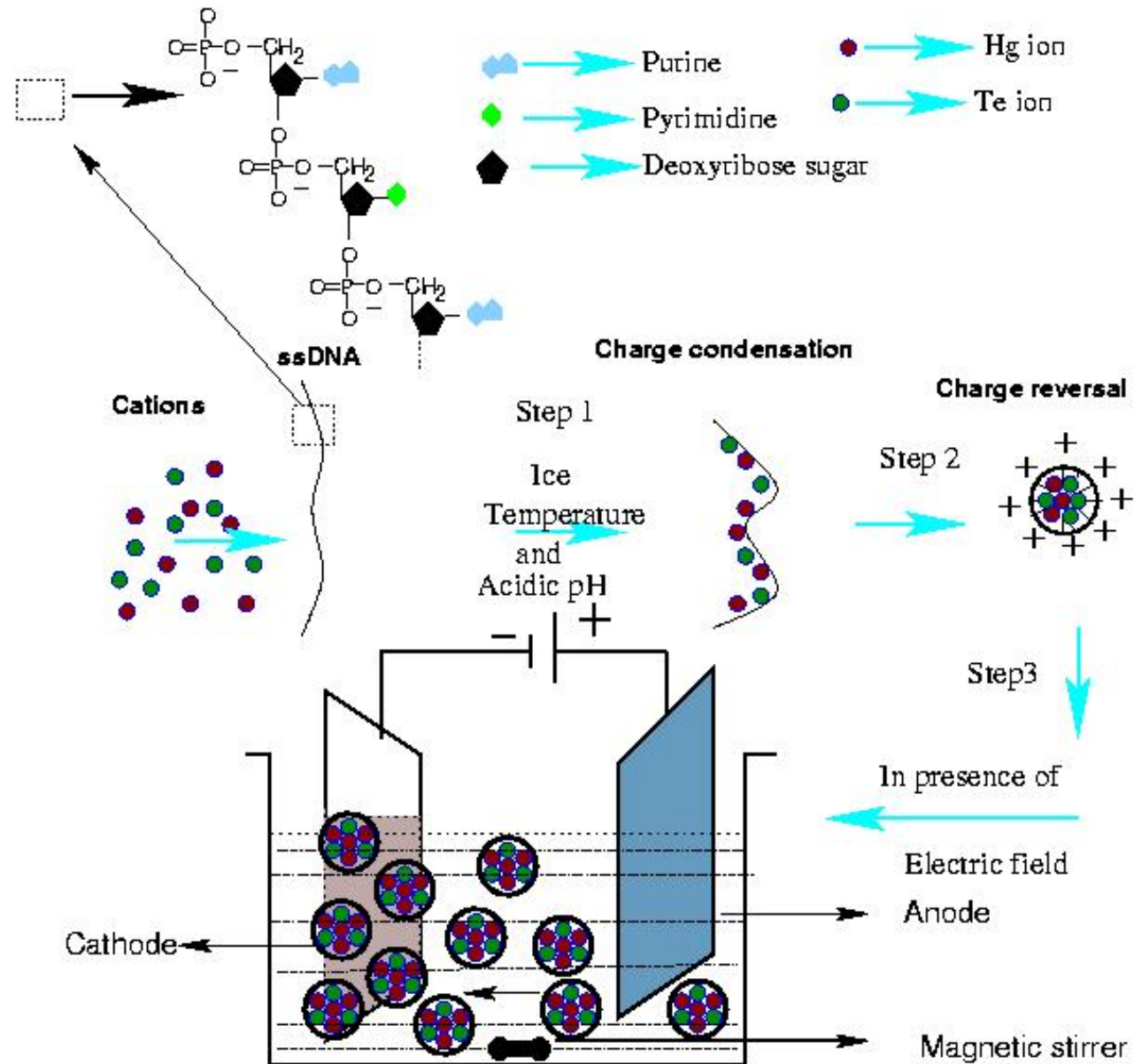


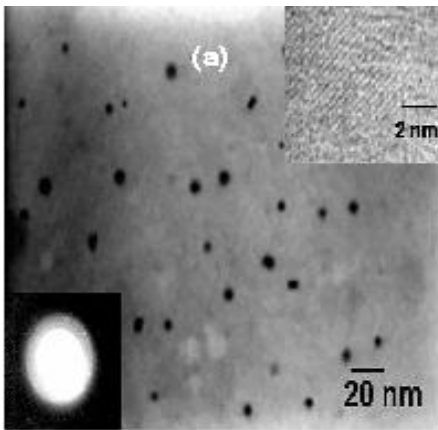
C-V characteristics : (a,b)-nano) and (c)-bulk



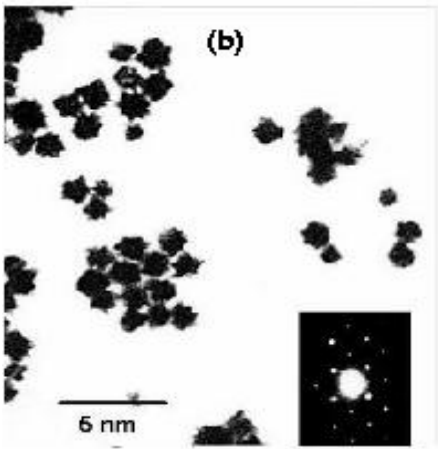
C-V characteristics of the
(a) low frequency
(b) high frequency

HgTe-DNA Nano-Bio systems

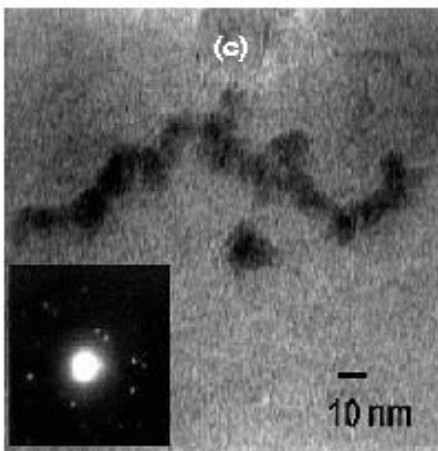




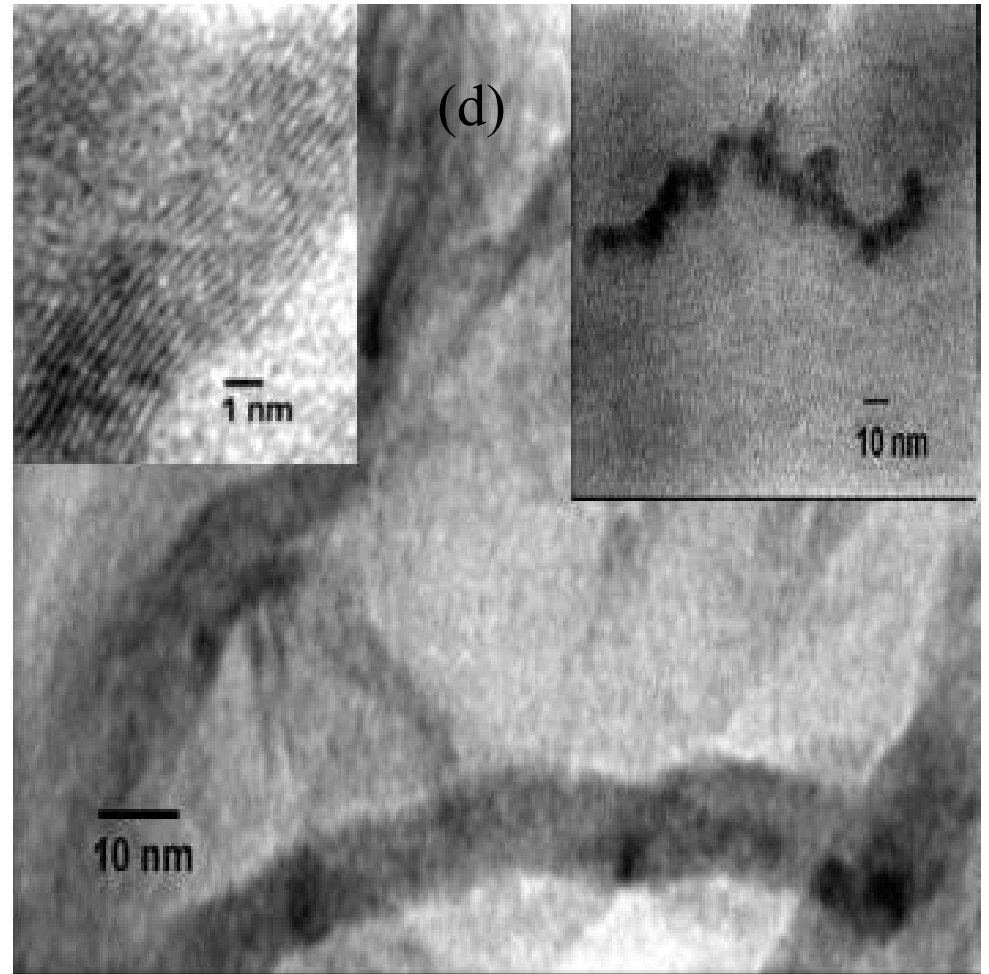
(a) TEM of Nano-HgTe.



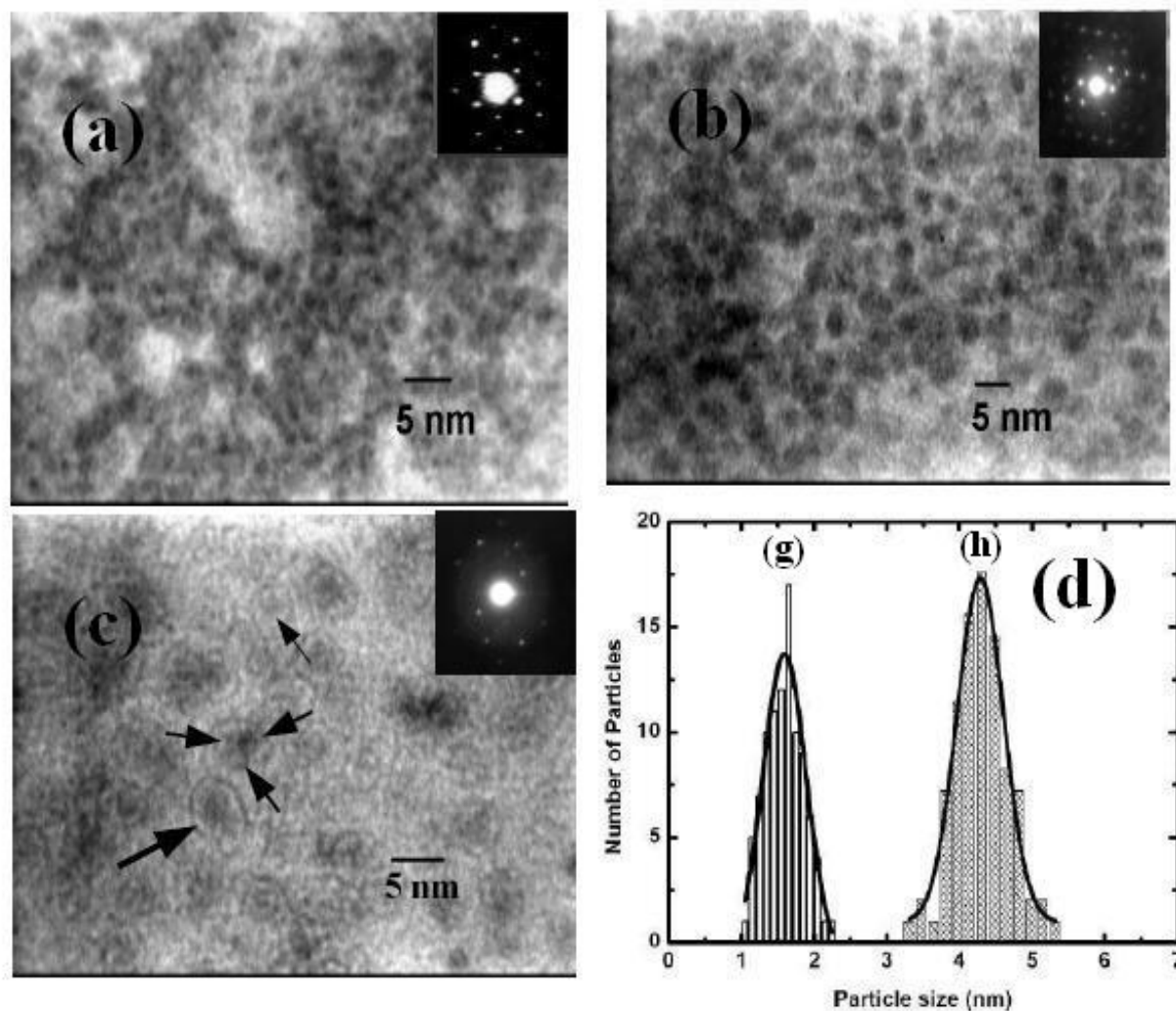
(b) TEM of
HgTe-ssDNA
cubic single
crystalline
Nanostars
ssDNA:
5'GCAAGCGGT
AACCAGTTGTTG 3'



(c) TEM of
HgTe-ssDNA
(Poly G-30)
String structure
Single crystalline
Sequence specific
interaction



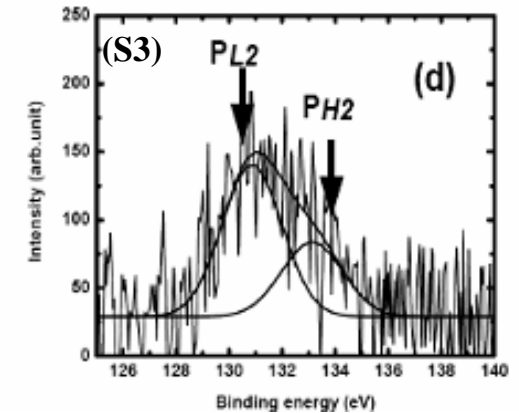
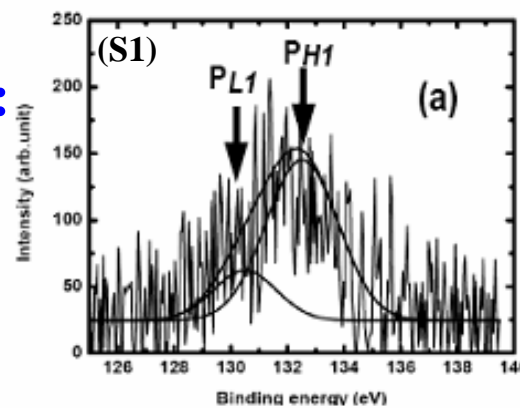
(d) TEM of
HgTe-DNA
(Poly G-30 + Poly C-30)
Nano wire of 4 nm width



TEM micrograph of HgTe – DNA hybrid QDs samples, S1 (a), S2 (b) and S3 (c). The insets in (a), (b) and (c) are the respective SAD patterns. (d) The size distribution plots of S1 (g) empty blocked and S2 (h) mosaic blocked histograms

Mechanism of DNA hybridization with cations and electronic structure:

Sample S1: HgTe-aDNA,
Sample S2: HgTe-bDNA
Sample S3: HgTe- aDNA-bDNA,
aDNA \rightarrow 5'GCAAGCGGTGAACCA
bDNA \rightarrow Conjugate of aDNA



P 2p core level XPS spectra of samples S1 and S3 which show a spin doublet structure

The standard P 2p level of DNA appear at 132.2 eV

OBSERVATIONS AND EXPLANATIONS:

1) P_{L1} & P_{L2} shifts to low B.E,

Shifting of PL1 and PL2 to low B.E suggests phosphoester bonding with Hg^{2+} & Te^{4+} . Electropositive host atom induces -ve charge to the neighbour atoms and destabilize the core level by coulomb repulsion. So, P_{L1} & P_{L2} shifts to low B.E for sample S1.

2) P_{H1} & P_{H2} shifts to higher B.E

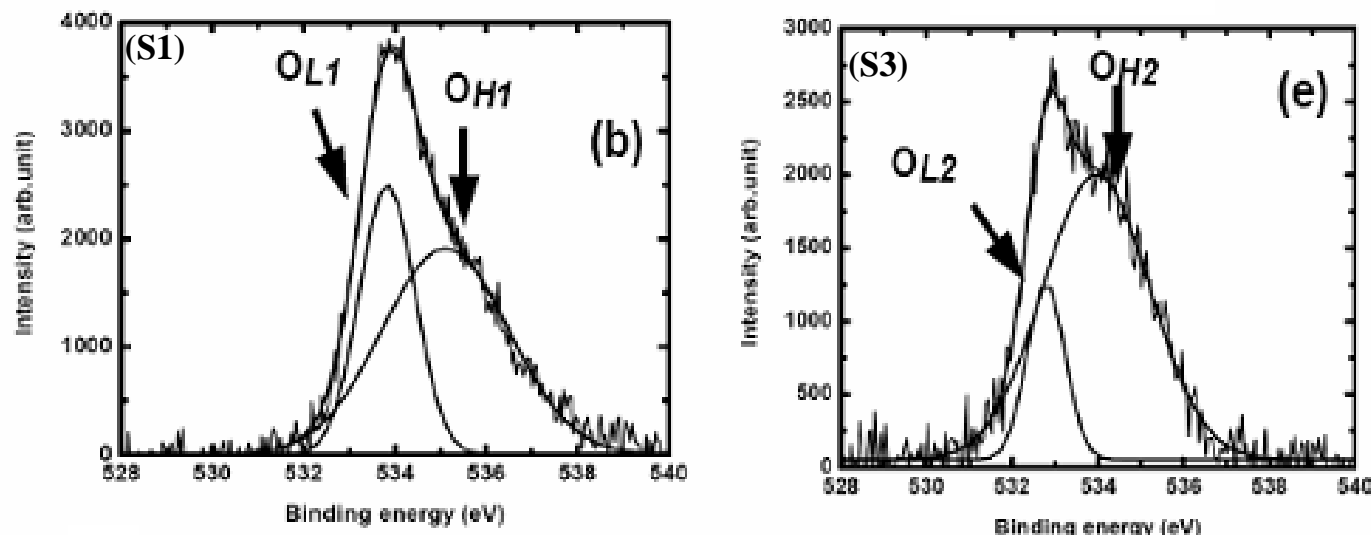
Shifting of P_{H1} & P_{H2} to higher B.E suggests simultaneous bonding of cations to -vely charged backbone forms a complex, responsible for self assembling process.

3) Relative intensities change,

In case of S1, electrostatic interaction and complex formation dominates over phosphoester linkage. For S3, the phosphoester linkage dominates over electrostatic interaction due to low availability of cations and suggests the equilibrium situation.

4) FWHM of PL & PH of S3 > S1

FWHM of $P_{H1} > P_{L1}$ in S1 suggest chemical reactivity of electrostatic interaction is fast during complex formation which give a compact structure. FWHM of P_{H2} & $P_{L2} >$ FWHM of P_{H1} & P_{L1} in case of S3 suggests chemical reactivity is more for S3 compared to S1 due to more availability of phosphate group.



Oxygen core level (O 1s) XPS spectra of S1 and S3 which show a satellite feature in higher B.E side.

The Oxygen core level of phosphate group of bare DNA appear at 531.0 eV. O_{L1} & O_{L2} , O_{H1} & O_{H2} peak positions are shifted to higher B.E.

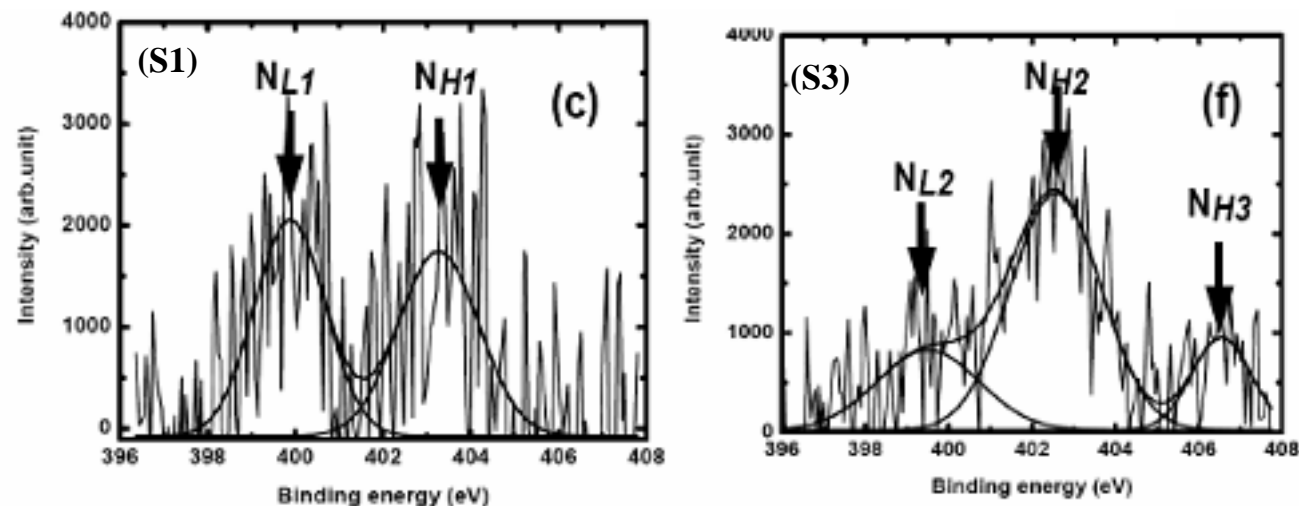
Interaction between negatively charged DNA backbone and cations is the dominate mechanism at the intial stages of sample synthesis.

More shift of O_{H1} & O_{H2} to higher B.E is due to two competitive mechanisms: electrostatic interaction with cations by phosphate group and phophoester bonding for complex formation.

For S1, intensity of $O_{L1} > O_{H1}$ suggest : Electrostatic interaction dominate phosphoester bonding

For S3, the relative intensity of $O_{L2} < O_{H2}$ suggest :

At initial stage, when aDNA is stabilized in the solution containing Hg^{2+} and Te^{4+} , it already forms a complex. When bDNA is added, due to less availability of cations, bDNA interacts with aDNA and provide the stability undergoing phophoester bonding and base-base interaction forming a duplex.

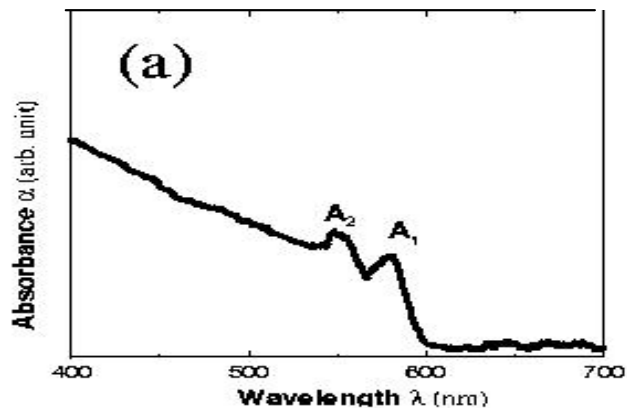


N 1s core level spectra of S1 & S3

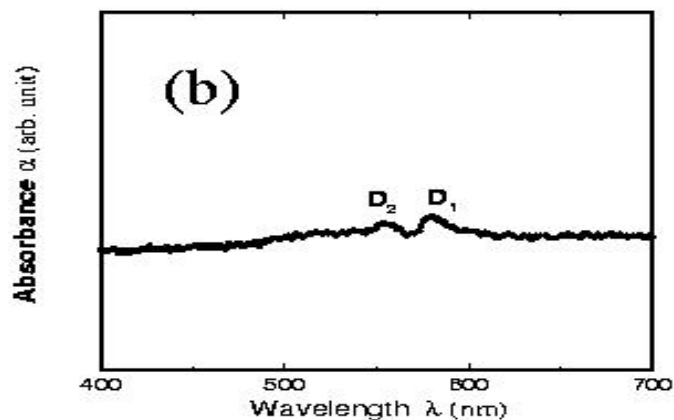
Bare N 1s level of DNA appear at 398.6 eV.

For S1, N_{LI} & N_{HI} shifts to higher B.E which corresponds to the resonance peak of double (- N =) and single (- N -) bonding nature of N. The shift is due to the formation of a super structure (circular quadruplex through covalent legation) in presence of multivalent cations for stability reasons.

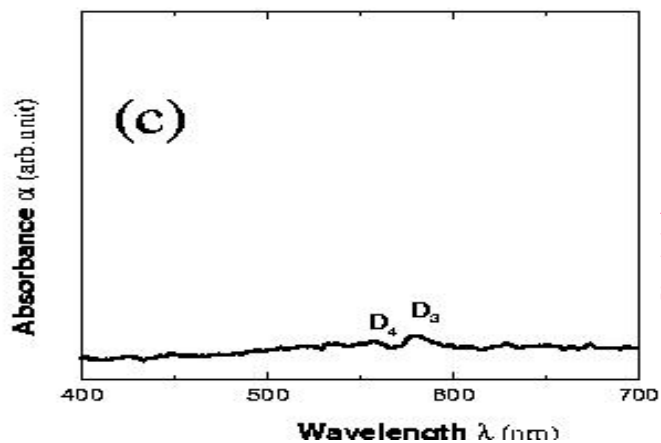
So, we see rapping of DNA around the HgTe QD.



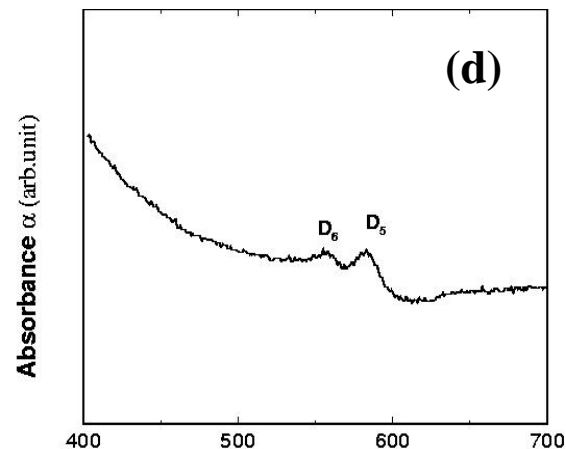
(a) Optical absorption of HgTe Ncs (average size ~ 5.35 nm). A1 and A2 correspond to the HHV-CB and LHV-CB transitions respectively.



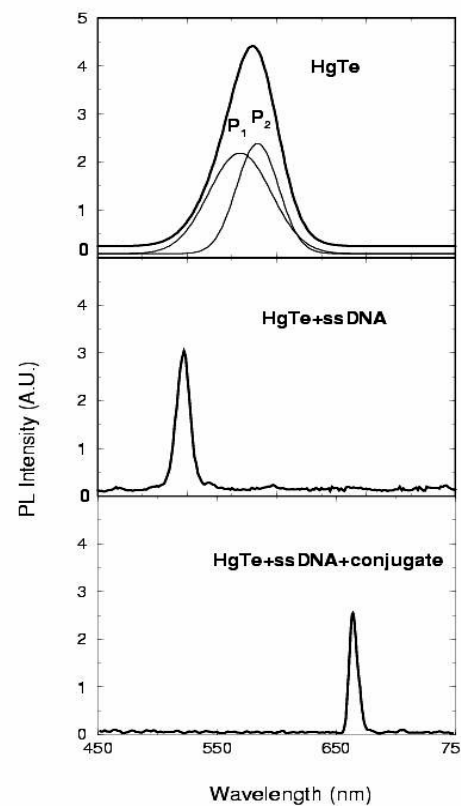
(b) Optical Absorption of HgTe-ssDNA (5'GCAAGCGTAACCAGTTG TTG 3') Complex NCs



(c) Optical Absorption of HgTe-ssDNA-conjugate ssDNA Complex NCs.



(d) Optical Absorption of HgTe-Poly-G(30) Complex NCs.

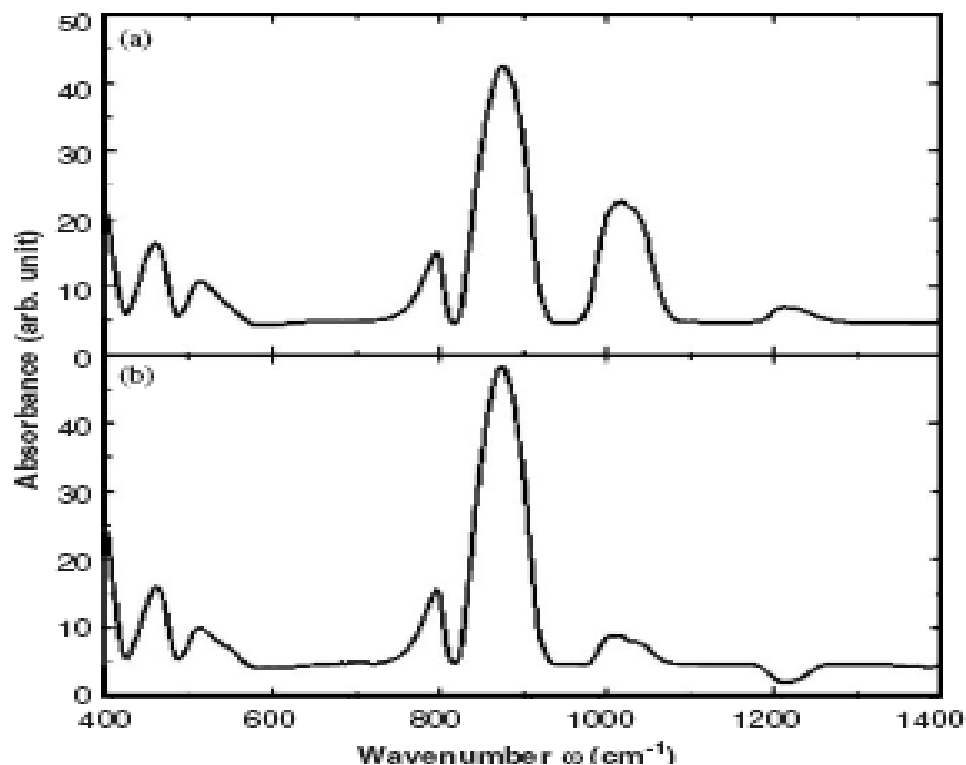


(a) PL of Nano-HgTe P1: Band Edge (579 nm) P2: Red Shifted band (588 nm)

(b) Blue shifted narrow Single PL peak (548 nm)

(c) Red shifted PL peak (662 nm) illustrates bio-sensing/ molecular recognition properties

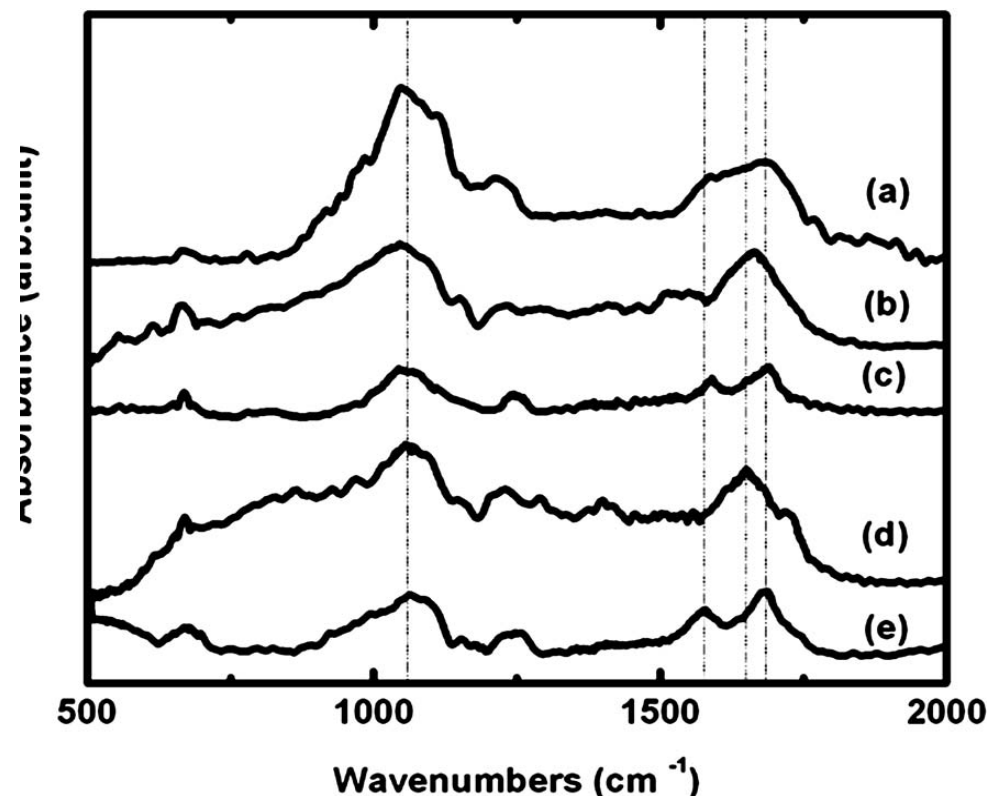
FTIR study of HgTe & DNA



FTIR spectra of

- (a) HgTe-ssDNA(5'GCAAGCGTAACCAGTTGTTG3') nanostars
(b) ssDNA (5'GCAAGCGTAACCAGTTGTTG3').

1016cm⁻¹ band Corresponds to Deoxyribose sugar Enhanced integral intensity of HgTe-ssDNA system due to rapping nature of ssDNA

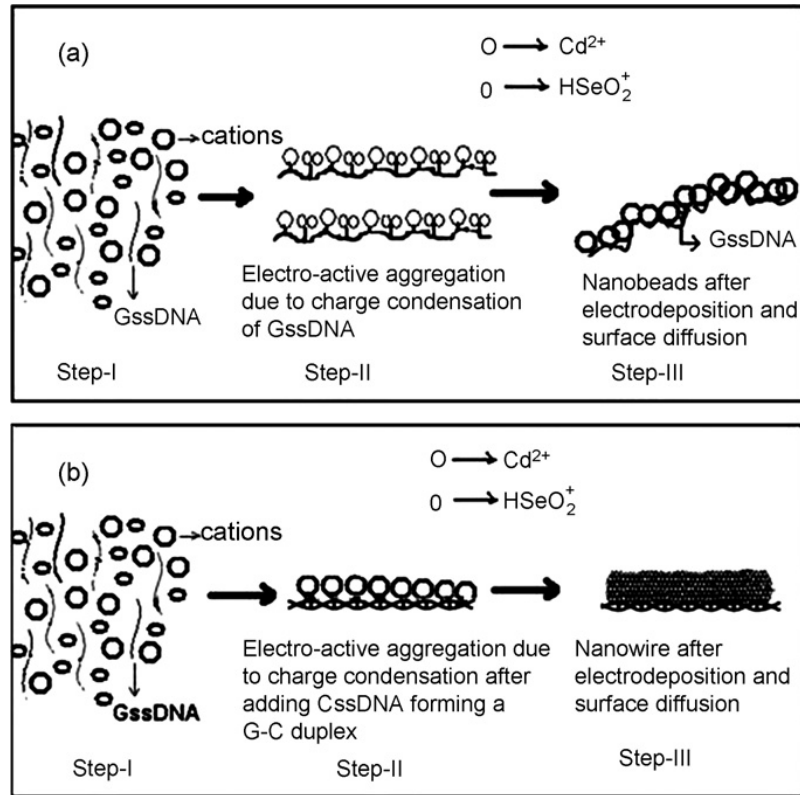


FTIR spectra of

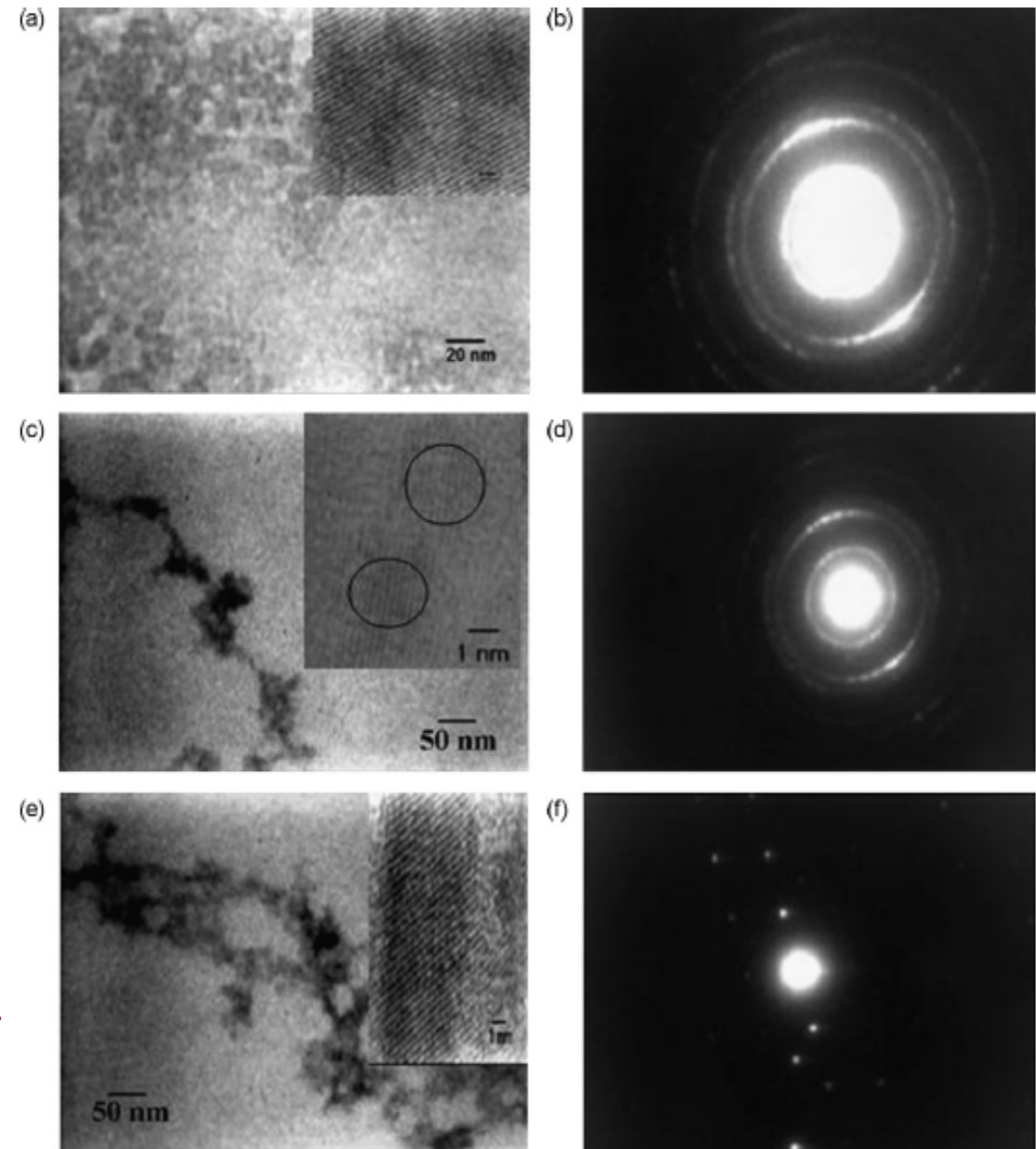
- (a) HgTe-ssDNA, Poly G(30)
(b) HgTe-ssDNA, Poly C(30)
(c) HgTe-ssDNA, Poly G(30)+ Poly C(30)
(d) ssDNA, Poly G(30)
(e) ssDNA, Poly C(30)

FTIR absorption peaks at 1043.30, 1590, and 1690.30 cm⁻¹ corresponds to the vibration of C-O-P sugar-phosphate bond of Poly G(30) backbone, C=N7 and C6=O bonds of Guanine and 1045.29 and 1666.19 cm⁻¹ are corresponding to the vibration of C-O-P sugar-phosphate bond of ssDNA backbone and C2=O bond of Cytosine, respectively

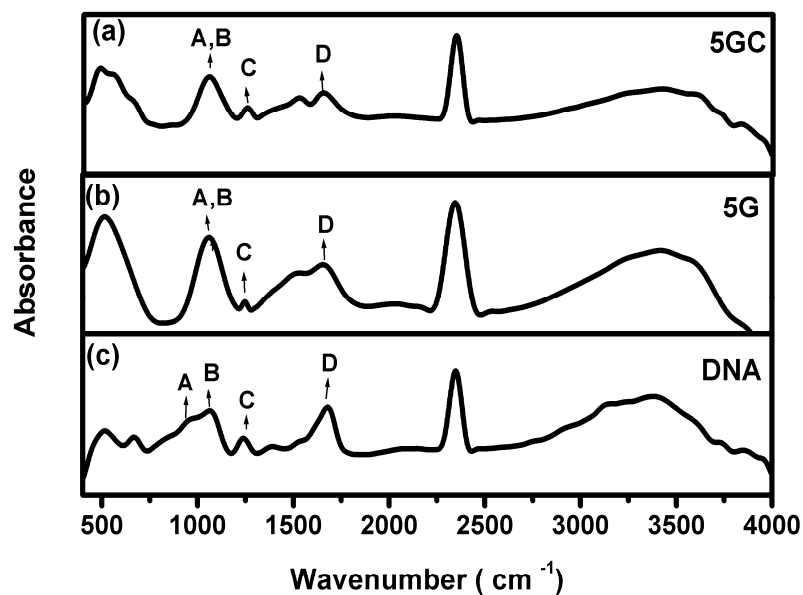
CdSe-DNA Nano-Bio systems



A schematic illustration of the method for fabrication of biocatalyst-mediated (a) NBs and (b) NWs growth

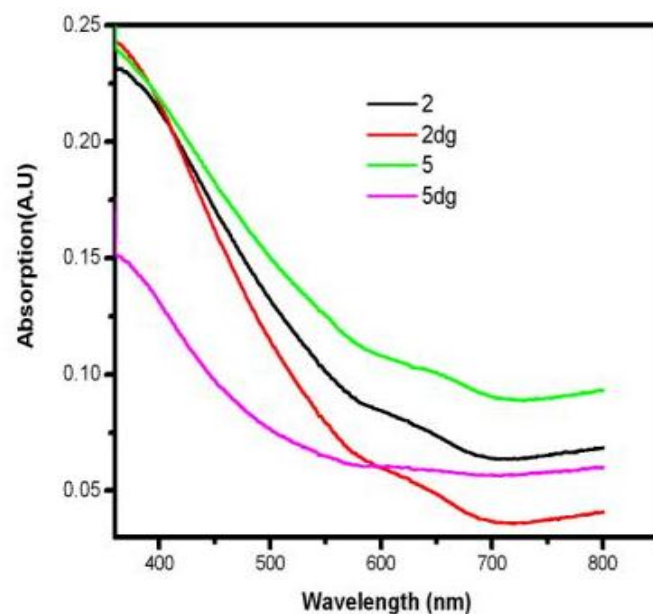


(a) TEM micrograph of CdSe NCs, (b) SAD of CdSe NCs
 (c) TEM micrograph of CdSe Nanobeads (d) SAD of CdSe Nanobeads
 (e) TEM of micrograph of CdSe Nanowires, inset is the lattice image of CdSe Nanowire (f) SAD of CdSe Nanowires.

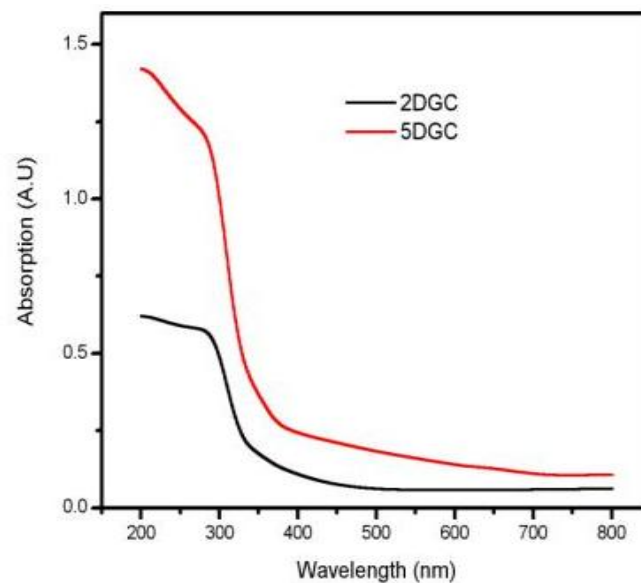


Fourier transforms infrared (FTIR) spectra of sample, (a) CdSe nanowires (b) of CdSe NBs and (c) DNA duplex.

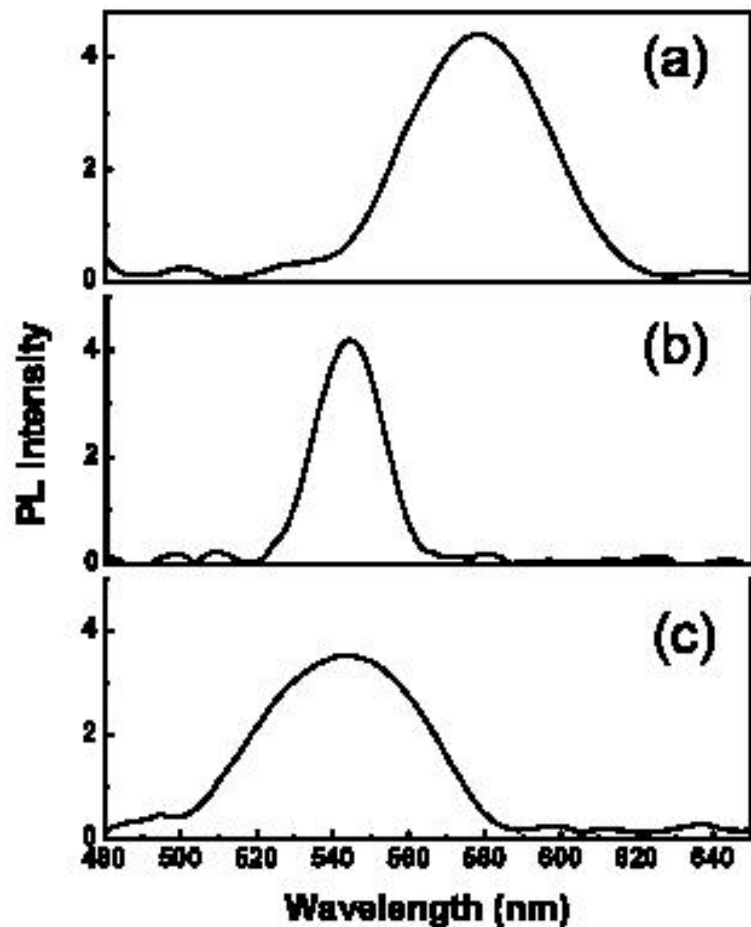
FTIR bands A, B, C, D at 968 cm^{-1} , 1050 cm^{-1} , 1229 cm^{-1} and 1690 cm^{-1} appear for CdSe nanobead (b) and CdSe Nanowires (a) which are shifted compared to bare DNA sample (a).



a) Absorption Spectra Of Nano-CdSe+ssDNA Poly G-30 Prepared at 2 mA/cm^2 And 5 mA/cm^2



b) Absorption Spectra Of Nano-CdSe+ssDNA+conjugate (Poly G-30, Poly C-30) Prepared at 2 mA/cm^2 And 5 mA/cm^2



The PL spectra of CdSe NCs (a), Nanobeads (b) Nanowires (c) taken at 300K.

The PL peak of CdSe NCs at 578 nm, FWHM = 20 nm. The PL peak of CdSe Nanobeads is at 544 nm, FWHM = 9.0 nm. Blue shift = 34 nm compared to CdSe NCs. PL intensity is quenched by 6% compared to CdSe NC sample.

The PL peak of CdSe Nanowire is at 544 nm, FWHM = 18 nm. PL intensity is quenched by 24 % compared to CdSe NCs and 22 % compared to CdSe Nanobeads. The PL quenching essentially amounts to the tagging of nanoparticles to DNA duplex indicative of the biomolecular recognition applications.

Such biomolecular recognition can also be achieved through conventional polymerized chain reaction (PCR) with the use of an organic dye. However, such PCR techniques, normally results a broad spectrum. Here is a technique, where the biomolecular recognition can be achieved spectroscopically but with better resolution.

Thank you